FEBS 24450 FEBS Letters 487 (2000) 239–247

Intercellular Ca^{2+} waves in rat hippocampal slice and dissociated glial–neuron cultures mediated by nitric oxide

Nicholas J. Willmott*, Kay Wong, Anthony J. Strong

Department of Clinical Neuroscience, Institute of Psychiatry, King's College London, De Crespigny Park, Denmark Hill, London SE5 8AF, UK

Received 2 November 2000; accepted 14 November 2000

First published online 8 December 2000

Edited by Maurice Montal

Abstract Nitric oxide (NO) may participate in cell–cell communication in the brain by generating intercellular Ca^{2+} waves. In hippocampal organotypic and dissociated glial–neuron (>80% glia) cultures local applications of aqueous NO induced slowly propagating intercellular Ca^{2+} waves. In glial cultures, Ca^{2+} waves and Mn^{2+} quench of cytosolic fura-2 fluorescence mediated by NO were inhibited by nicardipine, indicating that NO induces Ca^{2+} influx in glia which is dihydropyridine-sensitive. As NO treatments also depolarised the plasma membrane potential of glia, the nicardipine-sensitive Ca^{2+} influx might be due to the activation of dihydropyridine-sensitive L-type Ca^{2+} channels. Both nicardipine-sensitive intercellular Ca^{2+} waves and propagating cell depolarisation induced by mechanical stress of individual glia were inhibited by pretreating cultures with either an NO scavenger or N^G-methyl-L-arginine. Results demonstrate that NO can induce Ca^{2+} waves in hippocampal slice cultures, and that Ca^{2+} influx coupled to NO-mediated membrane depolarisation might assist in fashioning their spatio-temporal dynamics.

Key words: Nitric oxide; Glia; Astrocyte; Hippocampus; Calcium wave; Depolarisation

1. Introduction

Several underlying mechanisms have been proposed to account for complex spatio-temporal Ca^{2+} dynamics observed in cells and tissues [1]. In mixed glial–neuron cell cultures, intercellular Ca^{2+} waves that propagate through neighbouring cells are likely to be the result of combined contributions of intracellular and extracellular signalling pathways. The diffusion of Ca^{2+} mobilising second messengers (inositol-1,4,5-trisphosphate and Ca^{2+}) across gap junctions [2,3] and ATP release from cells resulting in P_2 receptor activation [4,5] are apparently involved in this process, but it is unlikely that these represent the sole mechanisms responsible for Ca^{2+} wave initiation and propagation [6].

Recently, we reported that nitric oxide (NO) mobilises Ca^{2+} from intracellular stores of glia via the NO-cGMP dependent protein kinase (NO-G-kinase) signalling pathway and that NO is an effective mediator of intercellular Ca^{2+} waves in dissociated glial–neuron cell cultures [6]. These data suggest that NO might participate in non-electrical cell–cell communication in the brain via the generation of propagating intercellular Ca^{2+} waves. To test our hypothesis further, we examined the effect of aqueous NO on the cytosolic Ca^{2+} concentration ($[Ca^{2+}]_i$) of cells in hippocampal organotypic slices. We also assessed whether NO-induced Ca^{2+} influx might play a role in the propagation of intercellular Ca^{2+} waves mediated by NO and by the mechanical stress of single glial cells, using dissociated mixed glial–neuron cultures as an appropriate model. Results from our study demonstrate that NO can generate slowly propagating intercellular Ca^{2+} waves in hippocampal organotypic slices and that Ca^{2+} influx coupled to NO-mediated plasma membrane (PM) depolarisation is a mechanism that is likely to assist Ca^{2+} wave propagation in the above culture systems.

2. Materials and methods

2.1. Preparation of dissociated glial–neuron cultures

Mixed glial–neuron primary cell cultures were prepared in a similar way as previously described [6]. Briefly, four forebrains of 1–2 day postnatal rats were dissected and transferred to Ca/Mg-free Hanks' balanced salt solution (HBSS) to which an equal volume of 0.25% trypsin/1 mM EDTA solution (Gibco) had been added. Forebrains were cut into small pieces and were incubated in this medium for 20 min at 37°C in a humidified atmosphere of 95% air, 5% CO_2. Forebrain pieces were transferred to a 15 ml conical centrifugation tube (Corning), and were washed with 4×10 ml aliquots of an equal mixture of Dulbecco's modified Eagle's medium (DMEM) and Ham's F-12. Finally, pieces were suspended in 3 ml of tissue culture medium consisting of 10% foetal calf serum and 90% of an equal mixture of DMEM and F-12, supplemented with 8 mg/ml D-glucose, 20 U/ml penicillin and 20 μg/ml streptomycin, and were triturated to homogeneity. Aliquots (100 μl) of the resulting cell suspension were overlaid onto zero thickness glass coverslips in six-well dishes, which had been precoated with poly-L-lysine (2.5 μg/coverslip) and laminin (5 μg/coverslip). Following a 3 h incubation at 37°C in a humidified atmosphere of 95% air, 5% CO_2, coverslips were flooded with 2 ml of the above tissue culture medium, and were maintained for 1–3 weeks in culture, prior to use. Every 3 days, 1 ml of culture medium was removed from coverslips and replaced with 1 ml of fresh culture medium.

2.2. Preparation of hippocampal slice cultures

Forebrain slices (300 μm thick) were prepared from 7 day old rats using a vibratome. During slice preparation forebrains were maintained in HBSS which was aerated with 95% O_2, 5% CO_2 at 22°C. Hippocampal regions were isolated from the 300 μm thick slices by dissection and were transferred to 0.02 μm Anopore membrane inserts (Nalge Nunc International) which were placed in six-well dishes, with each well containing 1 ml of culture medium. The culture medium was composed of Eagle's minimum essential medium (MEM) supple-

*Corresponding author. Present address: St. Bartholomew's and the Royal London School of Medicine and Dentistry, Queen Mary and Westfield College, Medical Sciences Building, Neuroscience Section, Room 2.22.19, Mile End Road, London E1 4NS, UK. Fax: (44)-20-7882 7726. E-mail: n.j.willmott@qmw.ac.uk

0014-5793/00/$20.00
PII: S0014-5793(00)02359-0

mented with 25% horse serum, 25% HBSS, 8 mg/ml D-glucose, 20 U/ml penicillin and 20 μg/ml streptomycin, pH 7.2. Hippocampal slices were maintained at 37°C in a humidified atmosphere of 95% air, 5% CO_2 for 3 days prior to use in order to allow them sufficient time to adhere to Anopore membranes.

2.3. Immunocytochemistry

Immunocytochemical stains for glial fibrillary acidic protein (GFAP) and neurofilament protein (NFP) were used to quantify the proportion of astrocytes to neurons in the pyramidal neuronal layer (PNL) of cultured hippocampal slices after 3 days and in dissociated glial–neuron cultures after 7 days. Anopore membrane inserts supporting adherent slices and coverslips with glial–neuron cultures were rinsed twice in HBSS (see drugs and solutions) at room temperature and were then fixed with 100% methanol at −20°C for 10 min. After two more washes in HBSS, slices and coverslips were blocked with 10% normal goat serum in phosphate-buffered saline (PBS) for 20 min at room temperature, and were then incubated overnight at 4°C with primary antibody (rabbit IgG anti-GFAP, 1:100, or rabbit anti-neurofilament-200, 1:100; Sigma) in 1% normal goat serum in PBS. Slices and coverslips were then washed three times in PBS at room temperature, and were incubated in the secondary antibody in PBS (Oregon Green™ 488-goat anti-rabbit, 1:50, Molecular Probes) for 45 min at room temperature. Glial–neuron cultures and the PNL of hippocampal slices were examined under epi-fluorescence using an Olympus BX50WI upright microscope, 40× water-immersion objective (LUMPlanFL40xW: 0.8 NA) and excitation light of 490 nm. Fluorescence images were captured with Axon Imaging Workbench software (Axon Instruments, CA, USA) using a 12-bit interline CCD (5 MHz Micromax: Roper Scientific, NJ, USA). Images were analysed using Corel Photo-Paint (Corel Corporation, USA).

2.4. Measurement of $[Ca^{2+}]_i$ in mixed glial–neuron cell cultures and hippocampal slice cultures

Intra and intercellular Ca^{2+} signalling was assessed in dissociated glial–neuron cultures after 7 days and in the PNL of hippocampal slice cultures after 3 days. After 7 days, glial–neuron cultures were predominantly composed of glia, as >80% of cells showed cross-reaction with antibody to GFAP. For these cultures, cells were loaded with Ca^{2+} indicator by incubation with 2 μM of the acetoxymethyl (AM) ester of fura-2 for 1 h. Intracellular fluorescence was imaged at 22°C in HBSS, using a 40× oil-immersion objective (1.3 NA) and inverted microscope (Nikon TMD), coupled to a xenon arc lamp/fast filter switching device (Sutter DG4: Sutter Instruments, CA, USA), and 12-bit interline CCD (5 MHz Micromax: Roper Scientific, NJ, USA) which were both interfaced to a Pentium II computer. Hippocampal slice cultures were loaded with Ca^{2+} indicator by incubation with 50 μM of fura-2 AM for 2.5 h and intracellular fluorescence was imaged at 22°C in HBSS using the same system as above apart from the microscope which was an upright Olympus BX50WI with a 20× water-immersion objective (UMPlanFL20xW: 0.5 NA). A low temperature (22°C) was used for Ca^{2+} imaging experiments as fura-2 readily compartmentalises into cellular organelles at higher, physiological temperatures in these preparations. All cultures were maintained in a static, open chamber throughout experiments. Free cytosolic Ca^{2+} was quantified by taking the ratio of fluorescence intensities at excitation wavelengths 340 and 380 nm, using an emission wavelength of 510 nm. Pairs of 340 and 380 nm images were captured every 2.5–3.0 s and ratio images were calculated using Axon Imaging Workbench software (Axon Instruments, CA, USA). Standard $CaCl_2$ solutions were used to calibrate the system for measurements with fura-2, and viscosity corrections were made [7]. Cellular Ca^{2+} response parameters were compared for statistical significance using Student's *t*-test for unpaired observations.

2.5. Assessment of Ca^{2+} influx in glial–neuron cultures by the manganese quench of cytosolic fura-2 fluorescence

Cell cultures were loaded with fura-2 as above. Manganese quench of glial cell cytosolic fura-2 fluorescence was monitored using an excitation wavelength of 360 nm, with a similar inverted microscope-based imaging system as for Ca^{2+} measurements. Fluorescence images were captured every 4 s. Mn^{2+} (0.1 mM) was added to the cell chamber, and the effect of bolus additions of aqueous NO or cellular mechanical stress on the Mn^{2+} quench of cytosolic fura-2 fluorescence was assessed in glial cells.

2.6. Monitoring PM potential with the voltage-sensitive dye $DiBAC_4(3)$

PM potential was monitored in glial–neuron cultures using the slow response voltage-sensitive dye, bis-(1,3-dibutylbarbituric acid) trimethine oxonol ($DiBAC_4(3)$). This anionic dye enters depolarised cells where it binds to lipid membranes and proteins resulting in an increase in fluorescence. Owing to its high negative charge, $DiBAC_4(3)$ is excluded from mitochondria and is therefore a selective reporter of PM potential. Cells were incubated with 1 μM $DiBAC_4(3)$ for 1 h prior to and also throughout experiments. Intracellular fluorescence was imaged at 22°C in HBSS, using the same inverted microscope system as for Ca^{2+} measurements. Cells were maintained in a static, open chamber throughout experiments. PM potential was monitored by ratioing the change in fluorescence intensity at an excitation wavelength of 490 nm with the initial fluorescence intensity at 490 nm ($\Delta F/F_0$), using an emission wavelength of 515 nm. Fluorescence images were captured every 2.5 s and ratio images were calculated using Axon Imaging Workbench software (Axon Instruments, CA, USA).

2.7. Calibration of intracellular $DiBAC_4(3)$ fluorescence versus membrane potential

Intracellular $DiBAC_4(3)$ fluorescence was calibrated versus membrane potential by a similar method, as previously described [8]. Following incubation of cells in normal HBSS containing 1 μM $DiBAC_4(3)$ for 1 h at 22°C, the calibration of intracellular $DiBAC_4(3)$ fluorescence was performed at 22°C in modified HBSS containing 10 μM of the monovalent cationophore gramicidin, 1 μM $DiBAC_4(3)$ and varying ratios of Na^+ and *N*-methyl-D-glucamine so that $[Na^+]+[N\text{-methyl-D-glucamine}] = 142$ mM. In calibration experiments these modified HBSS solutions were added stepwise to cells. For the 0 $[Na^+]_o$ calibration step of Fig. 1, $NaHCO_3$ was replaced with 10 mM HEPES in the modified HBSS. Fluorescence intensity expressed in relative terms towards the fluorescence measured under control conditions (in unmodified HBSS and representing the fluorescence of $DiBAC_4(3)$ at the resting membrane potential; F_{RMP}) was averaged for 30 glial cells following this protocol (Fig. 1a). In gramicidin-permeabilised cells, normalised fluorescence (F/F_{RMP}) increased linearly with $\log[Na^+]_o$, whereas in non-permeabilised cells varying $[Na^+]_o$ had a negligible effect on the intracellular fluorescence of $DiBAC_4(3)$. Assuming that after gramicidin permeabilisation the total intracellular concentration of permeant cations remains constant at approximately 147 mM during the recording period, then intracellular $DiBAC_4(3)$ fluorescence in altered Na^+_o solutions can be related to membrane potential using a simplified Goldman–Hodgkin–Katz equation in which the membrane potential is given by:

$$E_m = 58\log([Na^+]_o + [K^+]_o)/([Na^+]_i + [K^+]_i) \quad (1)$$

Plotting $\log(F/F_{RMP})$ versus membrane potential (Fig. 1b) yielded a straight line from which fluorescence data was calibrated.

2.8. Drugs and solutions

Experiments were performed in HBSS (pH 7.2), containing 137 mM NaCl, 5.4 mM KCl, 1.3 mM $CaCl_2$, 0.83 mM $MgSO_4$, 0.42 mM Na_2HPO_4, 0.44 mM KH_2PO_4, 4.2 mM $NaHCO_3$ and 5 mM glucose. For experiments carried out in nominally Ca^{2+}-free medium, $CaCl_2$ was omitted from the above, and 0.5 mM EGTA was added, yielding a free Ca^{2+} concentration of ~10 nM. NO gas was from Aldrich. Aqueous NO was prepared in HBSS and its concentration estimated according to a previously described method [9]. HAM's F-12 medium, DMEM, MEM, foetal calf serum, horse serum, penicillin and streptomycin were from Gibco (Glasgow, UK). Fura-2 AM and $DiBAC_4(3)$ were from Molecular Probes (CA, USA). N^G-methyl-L-arginine (L-NMMA) and 2-phenyl-4,4,5,5-tetramethyl-imidazoline-1-oxyl 3-oxide (PTIO) were from Calbiochem. All other drugs and sera were from Sigma (Poole, UK).

3. Results

3.1. NO-mediated PM depolarisation, Ca^{2+} influx and intercellular Ca^{2+} waves in dissociated glial–neuron cultures

After 7 days in culture, dissociated glial–neuron cultures were predominantly composed of glia, as >80% of cells

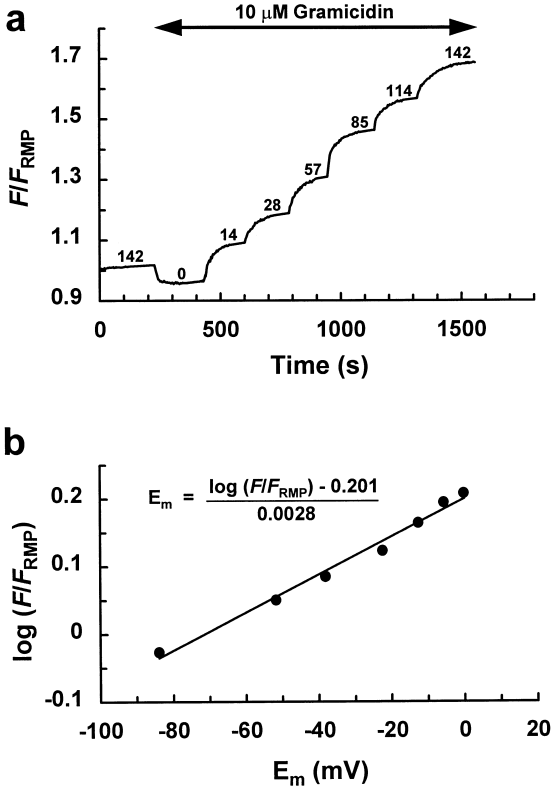

Fig. 1. Calibration of intracellular $DiBAC_4(3)$ fluorescence versus PM potential. (a) The calibration of intracellular $DiBAC_4(3)$ fluorescence was performed at 22°C in modified HBSS containing 10 μM gramicidin, 1 μM $DiBAC_4(3)$ and varying ratios of Na^+ and *N*-methyl-D-glucamine so that $[Na^+]+[N\text{-methyl-D-glucamine}] = 142$ mM. In calibration experiments these modified HBSS solutions were added stepwise to cells. Normalised intracellular fluorescence (F/F_{RMP}) of 30 cells was averaged following this protocol and a typical averaged trace is shown in (a) (the $[Na^+]_o$ in mM is indicated above each step). (b) The log of fluorescence data shown in (a) plotted versus the corresponding values of PM potential (E_m) calculated from the simplified Goldman–Hodgkin–Katz equation (Eq. 1). Data points in (b) are the mean of four separate experiments in different coverslips and the equation for the line of best fit by linear regression analysis is indicated.

showed cross-reaction with antibody to GFAP. It was possible to discriminate between glial and neuronal cells in our mixed glial–neuron cultures. Neuronal cells, which cross-reacted with antibody to NFP, were rounder in shape with fewer processes, and appeared phase bright under microscope illumination compared to glia. These differences assisted our selection of cells in mechanical stimulation experiments, where only individual glial cells were mechanically stressed. Also in subsequent experiments only glial cell PM potential was analysed in mixed glial–neuron cultures. Cell regions (350×300 μm) imaged in experiments contained upwards of 200 glial cells which were distributed evenly throughout the imaged area. Local application of a puff of aqueous NO onto these cultures using a microinjection pipette and picospritzer (WPI PicoPump PV820) resulted in the generation of an intercellular Ca^{2+} wave (Fig. 1a). This wave was characterised by a slow concentric propagation of increased $[Ca^{2+}]_i$ through neighbouring cells (propagation rate: 7.8 ± 1.2 μm/s, mean ± S.D.). In these puff experiments, the microinjection pipette containing aqueous NO at a concentration of 35 μM, was positioned centrally, at a distance of 80 μm above the cells. Puff duration was 50 ms, resulting in a reproducible delivery of 30 pl (calibrated by measuring injected droplet size in oil). By the same procedure, puffing solely HBSS onto cells did not affect $[Ca^{2+}]_i$.

The pre-treatment of cells with 10 μM nicardipine for 5 min resulted in both a reduction in $\Delta[Ca^{2+}]_i$ of individual cells (Fig. 1a,c) and also intercellular Ca^{2+} wave propagation rate (Fig. 1a,d), following a puff of aqueous NO, suggesting that a dihydropyridine-sensitive Ca^{2+} influx contributes to the NO-induced increase in $[Ca^{2+}]_i$. The extent of intercellular Ca^{2+} wave propagation was also affected by nicardipine pre-treatment, with waves usually restricted to coverslip areas of between 1 and 2×10^4 μm^2, as opposed to $3–5\times10^4$ μm^2 for untreated control cells. Further evidence for NO inducing Ca^{2+} influx in glial cells was derived from Mn^{2+} quench experiments. It is generally accepted that Mn^{2+} can enter cells along with Ca^{2+} via store-operated Ca^{2+} channels, which open following Ca^{2+} store depletion, and also probably via other Ca^{2+} or non-selective cation channels. Bolus application of 2 μM aqueous NO to cells resulted in Mn^{2+} quench of cytosolic fura-2 fluorescence (Fig. 1e), which was almost completely prevented by pre-treating cells with 10 μM nicardipine for 10 min (centre trace of Fig. 1e). These data suggest that a dihydropyridine-sensitive Ca^{2+} influx mechanism contributes to the propagation of NO-mediated intercellular Ca^{2+} waves.

Considering that NO depletes intracellular Ca^{2+} stores of glia [6], it is possible that store-operated Ca^{2+} influx, or an influx mechanism activated by an increase in $[Ca^{2+}]_i$ might be implicated in the response to NO. NO-mediated Ca^{2+} influx might also be explained by NO inducing PM depolarisation resulting in the activation of dihydropyridine-sensitive L-type Ca^{2+} channels. To test this latter hypothesis, we applied NO to cultures bathed in the presence of the slow response voltage-sensitive dye $DiBAC_4(3)$. Following application of a puff of aqueous NO, we observed an increase in intracellular fluorescence in glia, indicative of PM depolarisation (Fig. 1b,f). NO itself did not increase the fluorescence of $DiBAC_4(3)$, as puffing aqueous NO into 50 mM of the dye (in dimethyl sulfoxide (DMSO)) resulted in transient fluorescence quenching (Fig. 1f). Transferring cultures to a nominally Ca^{2+}-free medium (0 Ca^{2+}, 0.5 mM EGTA) for 15 min resulted in the depletion of intracellular Ca^{2+} stores as the addition of 1 μM ionomycin to cells following this incubation period resulted in an increase in $[Ca^{2+}]_i$ of only 150 nM as opposed to 500–600 nM for cells challenged with ionomycin 30 s after being transferred to this Ca^{2+} chelating medium (data not shown). Incubating cells for 15 min in this nominally Ca^{2+}-free medium did not however affect the increase in intracellular $DiBAC_4(3)$ fluorescence induced by a puff of NO (Fig. 1f), indicating that NO-mediated PM depolarisation is probably Ca^{2+} independent.

3.2. *Evidence that propagating Ca^{2+} waves and PM depolarisation induced by mechanical stimulation of individual glial cells require NO*

Mechanical stimulation of a single glial cell evoked an intercellular Ca^{2+} wave in dissociated glial–neuron cultures (Fig. 2a). This was achieved by slowly lowering a microinjection pipette onto a centrally located, single glial cell. After touching the cell, the pipette was immediately removed. The resulting stress-induced intercellular wave was also characterised by concentric propagation of increased $[Ca^{2+}]_i$ through

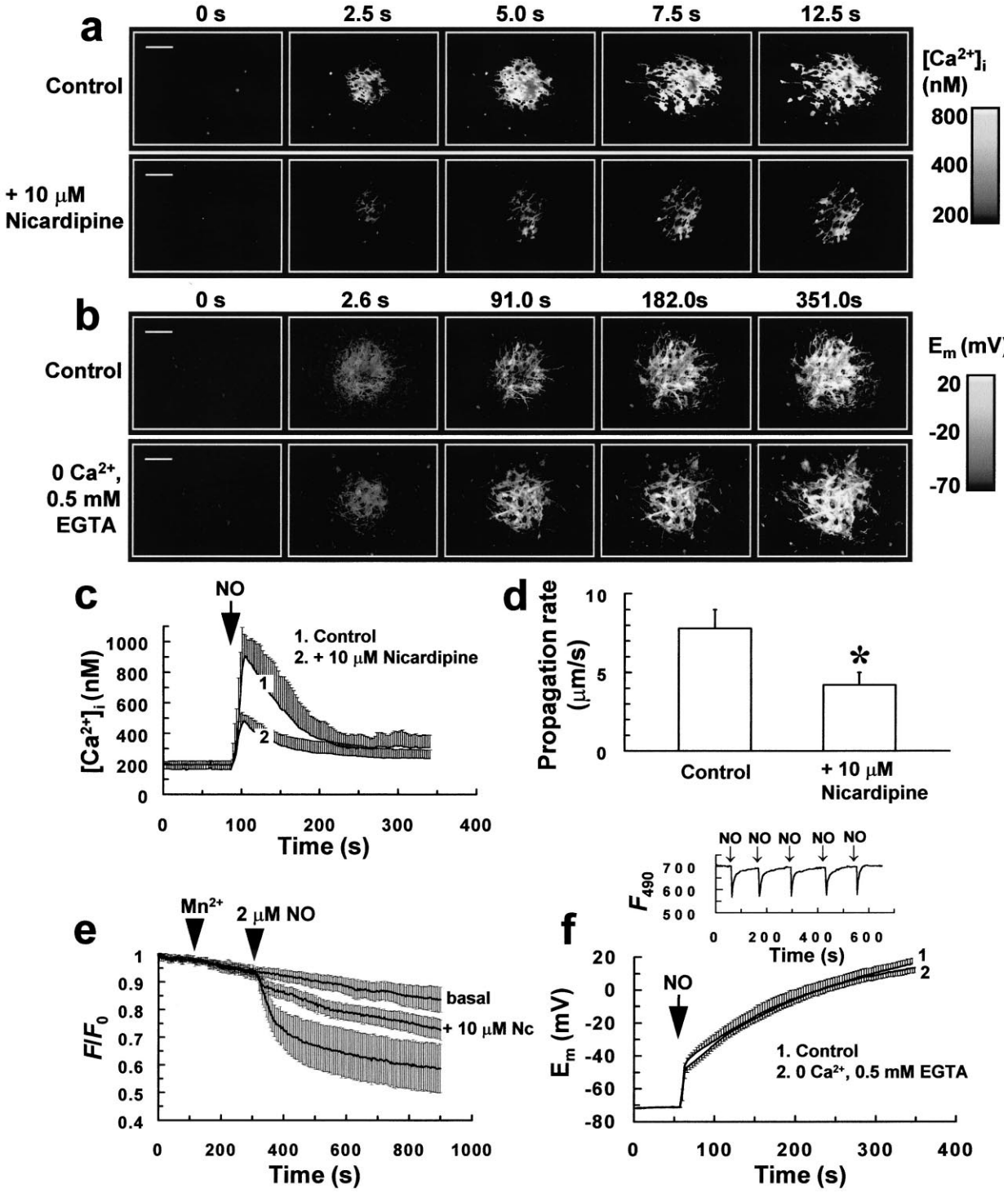

neighbouring cells (propagation rate: 13.3 ± 0.5 μm/s, mean ± S.D.). Pre-treating cells with the NO scavenger PTIO (100 μM) for 10 min, or the NO synthase (NOS) inhibitor L-NMMA (300 μM) for 30 min prior to mechanical stimulation resulted in a reduction in $\Delta[Ca^{2+}]_i$ and Ca^{2+} wave propagation rate (Fig. 2a,c,d), indicating that an NO-induced increase in $[Ca^{2+}]_i$ is likely to contribute to the stress-induced Ca^{2+} wave, as previously reported [6]. Dihydropyridine-sensitive Ca^{2+} influx was also implicated in the response as pre-treating cells with 10 μM nicardipine for 10 min also resulted in a reduction in $\Delta[Ca^{2+}]_i$ (Fig. 2c), Ca^{2+} wave propagation rate (Fig. 2d) and Mn^{2+} quench of cytosilic fura-2 fluorescence (Fig. 2e), following mechanical stimulation of a single glial cell. The extent of intercellular Ca^{2+} wave propagation was also affected by the above drug treatments, with waves usually restricted to coverslip areas of between 1 and 2×10^4 μm^2, as opposed to 5–6×10^4 μm^2 for untreated control cells.

Mechanical stimulation of a single glial cell also evoked an increase in intracellular $DiBAC_4(3)$ fluorescence which propagated slowly outwards from the target cell to eventually in-

Fig. 2. NO induces PM depolarisation, Ca^{2+} influx and intercellular Ca^{2+} waves in glial–neuron cultures. (a) Top panel (control): fluorescence ratio image sequence of a culture loaded with fura-2, showing a slowly propagating intercellular Ca^{2+} wave induced by puffing aqueous NO onto cells at $t=0$ s. The pipette concentration of NO was 35 μM, and puff duration was 50 ms, resulting in a reproducible delivery of 30 pl. Lower panel of (a) is the same as above, except cells were incubated with 10 μM nicardipine for 10 min prior to NO application which partially inhibited the NO-mediated Ca^{2+} wave. (b) Top panel (control): fluorescence ratio image sequence of glial–neuron cultures incubated with $DiBAC_4(3)$ showing an increase in the estimated PM potential (E_m) indicative of PM depolarisation, and mediated by a puff of NO at $t=0$ s. In the lower panel of (b), cells were transferred to a Ca^{2+} chelating medium (0 Ca^{2+}, 0.5 mM EGTA) for 15 min prior to NO application. Image sequences in (a) and (b) are representative of four separate experiments in different coverslips and scale bars are 50 μm. (c) $[Ca^{2+}]_i$ of 25 randomly selected glial cells that demonstrated an increase in $[Ca^{2+}]_i$ in response to NO was averaged for individual experiments of (a), with displayed traces representing the mean of these averaged responses from at least four separate experiments for untreated control, and nicardipine-treated cultures (error bars represent S.D.). (d) Propagation rate of the NO-induced intercellular Ca^{2+} wave in untreated control and nicardipine-treated cultures. Bars in (d) represent the mean of four separate experiments with error bars representing S.D. ($^*P<0.05$ versus control value; Student's t-test for unpaired observations). (e) Bolus application of 2 μM aqueous NO to cells resulted in Mn^{2+} quench of cytosolic fura-2 fluorescence, which was abrogated by pre-treating cells with 10 μM nicardipine (Nc; centre trace) for 10 min. All traces in (e) represent the mean normalised fluorescence intensity (F/F_0) of at least 200 cells from four separate experiments. Error bars represent S.D. For measurements of basal Mn^{2+} quench (top trace in e) no drugs were added to cells. (f) Estimated PM potential (E_m) of 25 randomly selected glial cells that demonstrated an increase in intracellular $DiBAC_4(3)$ fluorescence in response to NO was averaged for individual experiments of (b), with displayed traces representing the mean of these averaged responses from four separate experiments for untreated control cultures, and cultures transferred to a Ca^{2+} chelating medium (0 Ca^{2+}, 0.5 mM EGTA) for 15 min prior to NO application (error bars represent S.D.). Inset of (f) shows transient fluorescence quenching induced by repeatedly puffing NO into 50 mM $DiBAC_4(3)$ (in DMSO).
←

volve 50–100 cells distributed over coverslip areas of between $4–5\times10^4$ μm^2 (Fig. 2b). As $DiBAC_4(3)$ is a slow response voltage-sensitive dye, the spatio-temporal dynamics of the increase in intracellular $DiBAC_4(3)$ fluorescence are not comparable to the propagation of the stress-induced intercellular Ca^{2+} wave. This apparent stress-induced propagating depolarisation was almost completely abrogated by pre-treating cells with 100 μM PTIO for 10 min or 300 μM L-NMMA for 30 min (Fig. 2b,f) with only the target cell and typically less than 10 neighbouring cells (distributed over a coverslip area of less than 1×10^4 μm^2), demonstrating an increase in intracellular $DiBAC_4(3)$ fluorescence 350 s after mechanical stimulation (Fig. 2b). Considering that increases in $[NO]_i$ have previously been shown to be closely coupled to increases in $[Ca^{2+}]_i$ [6] due to the presence of Ca^{2+}-dependent NOS in glia [10], our combined data suggest that Ca^{2+} influx coupled to NO-mediated PM depolarisation is likely to facilitate the propagation of the stress-induced intercellular Ca^{2+} wave in glia.

3.3. NO-induced intercellular Ca^{2+} waves in hippocampal organotypic slices

After 3 days in culture, immunocytochemical stains for GFAP and NFP were used to quantify the proportion of glia to neurons, respectively, in the PNL of hippocampal organotypic slices (Fig. 3a,b,c) which was the region analysed in experiments. Neuronal cells, which cross-reacted with antibody to NFP (Fig. 3c), were rounder in shape and were approximately half as abundant compared to glia (Fig. 3b), indicating that cultured slices had retained a normal cellular architecture in the PNL.

In hippocampal organotypic slices loaded with the ratiometric Ca^{2+} indicator fura 2, cells in the surface layers of the PNL exhibited characteristic increases in $[Ca^{2+}]_i$ to bolus applications of glutamate and ATP (Fig. 3d,e,f) comprising of single transients and oscillations (Fig. 3e,f), indicative of normal Ca^{2+} signalling in these cultures. Following application of a localised bolus of aqueous NO (1.74 μM final concentration) to the medium bathing slices, we observed intercellular Ca^{2+} waves that propagated slowly through the PNL (Fig. 4a). The final NO concentration employed in our experiments (1.74 μM) is comparable to the basal extracellular levels of the NO breakdown products, nitrate (NO_3^-) and nitrite (NO_2^-), which have previously been estimated in rat striatum by microdialysis [11]. As for cells in dissociated glial–neuron cultures, the majority of cells in the PNL of hippocampal slices demonstrated transient increases in $[Ca^{2+}]_i$ in response to NO, albeit of a lower magnitude, with a $\Delta[Ca^{2+}]_i$ of between 100 and 200 nM (Fig. 4b). The propagation rate of the NO-mediated Ca^{2+} wave was a constant 28 ± 1.8 μm/s (mean ± S.D.) and was approximately 3.5-fold faster than the rate of NO-mediated waves that we measured in dissociated glial–neuron cultures (Fig. 4c). It is possible that the higher propagation rate observed in the PNL of our hippocampal slices might be a reflection of either a higher proportion of neurons to glia, or closer cell packing compared to our dissociated glial–neuron cell cultures, or may simply be due to an NO concentration dependency for wave propagation. These data demonstrate that as for predominantly glial cultures, NO induces propagating intercellular Ca^{2+} waves in hippocampal organotypic slices (Fig. 5).

4. Discussion

Results from this study suggest that Ca^{2+} influx coupled to NO-mediated PM depolarisation is likely to be an important mechanism that facilitates the propagation of intercellular Ca^{2+} waves in glia. We previously showed that NO also mobilises Ca^{2+} from ryanodine receptor-linked intracellular Ca^{2+} stores via the NO-G-kinase signalling pathway in these cells [6]. However, it is unlikely that Ca^{2+} release and an increase in $[Ca^{2+}]_i$ are involved in NO-mediated PM depolarisation as transferring cells to a Ca^{2+} chelating medium which resulted in Ca^{2+} store depletion did not affect the increase in intracellular $DiBAC_4(3)$ fluorescence following a puff of NO (Fig. 1b,f). Consequently, it is not apparent from our study how NO depolarises the PM potential of glial cells. Previous studies have shown that aqueous NO, NO donors and cGMP cause a depolarisation of PM potential in rat thalamic [12] and paraventricular nucleus neurons [13]. An NO donor has also been shown to induce membrane depolarisation in mouse cerebral cortical neurons resulting in L-type Ca^{2+} channel activation [14] which is potentially similar to our observations in glial cells. In our experiments, both control puffs of aqueous NO and mechanical stress of individual glia which stimulates NO production within cells [6] induce an increase in glial membrane potential from −71 mV to at least −30 mV.

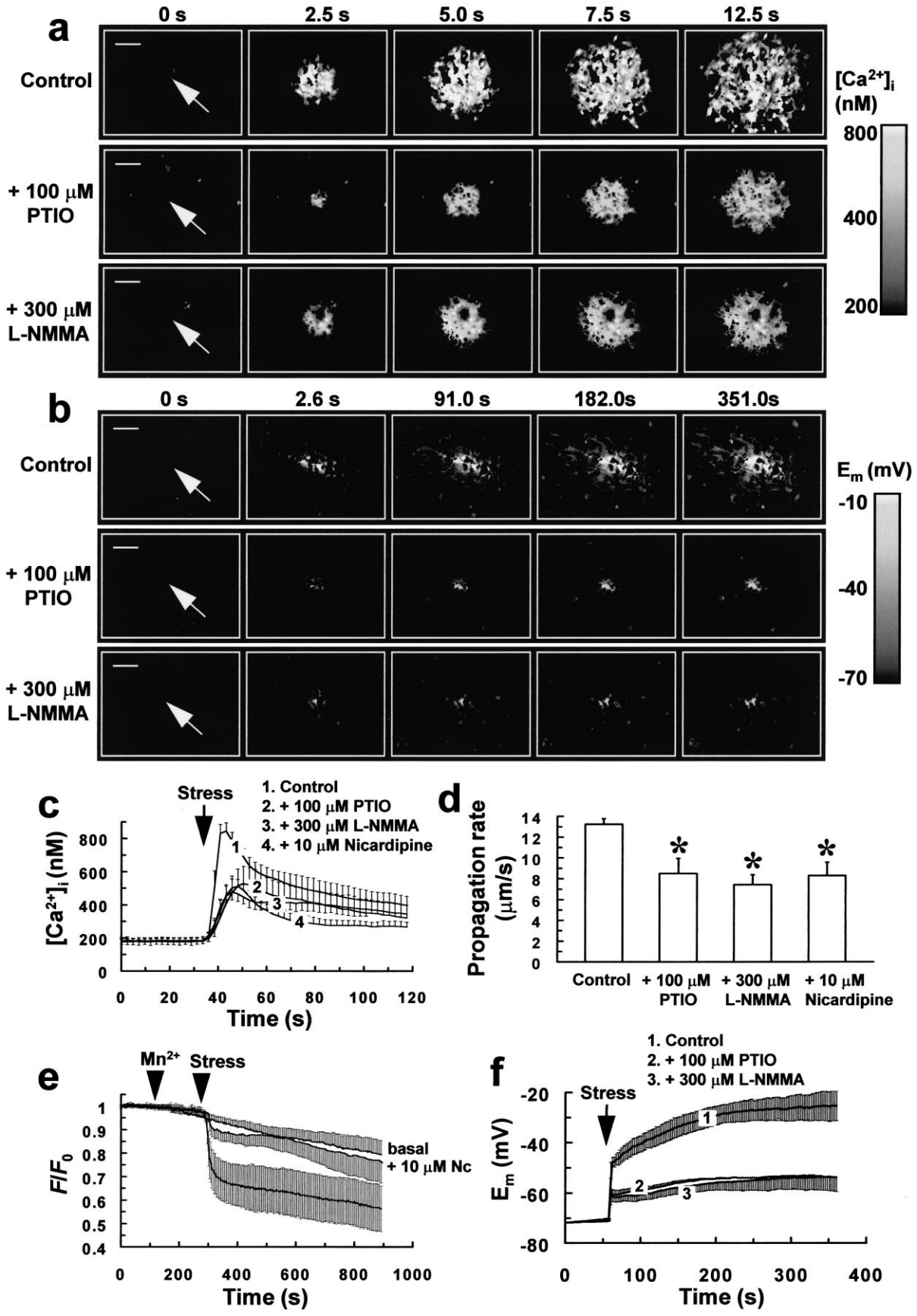
a
0 s
2.5 s
5.0 s
7.5 s
12.5 s
Control
+ 100 μM PTIO
+ 300 μM L-NMMA
[Ca2+]i (nM)
800
400
200
b
0 s
2.6 s
91.0 s
182.0s
351.0s
Control
+ 100 μM PTIO
+ 300 μM L-NMMA
Em (mV)
-10
-40
-70
c
Stress
1. Control
2. + 100 μM PTIO
3. + 300 μM L-NMMA
4. + 10 μM Nicardipine
[Ca2+]i (nM)
Time (s)
d
Propagation rate (μm/s)
Control
+ 100 μM PTIO
+ 300 μM L-NMMA
+ 10 μM Nicardipine
e
Mn2+
Stress
F/F0
basal
+ 10 μM Nc
Time (s)
f
1. Control
2. + 100 μM PTIO
3. + 300 μM L-NMMA
Stress
Em (mV)
Time (s)

Fig. 3. Propagating intercellular Ca^{2+} waves and PM depolarisation induced by mechanical stress of single glial cells in glial–neuron cultures are inhibited by PTIO and L-NMMA. Pre-treating cells with 100 μM PTIO for 10 min, or 300 μM L-NMMA for 30 min resulted in a reduction in both $\Delta[Ca^{2+}]_i$ of individual cells (a,c), the propagation rate of the intercellular Ca^{2+} wave (a,d) and the propagation of PM depolarisation estimated in cells incubated with $DiBAC_4(3)$ (b) following mechanical stress of single glial cells (arrowed). Fluorescence ratio image sequences in (a) and (b) are representative of four separate experiments for control and drug-treated cultures. Scale bars are 50 μm. (c) $[Ca^{2+}]_i$ of 25 of the closest glial cells to the mechanically stressed target cell that demonstrated an increase in $[Ca^{2+}]_i$ was averaged for individual experiments of (a) and for cultures pre-treated with 10 μM nicardipine for 10 min prior to mechanical stress, with displayed traces representing the mean of these averaged responses from at least four separate experiments for untreated control and drug-treated cultures (error bars represent S.D.). (d) Propagation rates of the stress-induced intercellular Ca^{2+} wave in untreated control and drug-treated cultures. Bars in (d) represent the mean of four separate experiments with error bars representing S.D. ($^*P < 0.05$ versus control value; Student's t-test for unpaired observations). (e) Mechanical stress of a single glial cell resulted in Mn^{2+} quench of cytosolic fura-2 fluorescence (estimated in 25 of the closest cells to the mechanically stressed target cell) in neighbouring cells, which was abrogated by pre-treating cultures with 10 μM nicardipine (Nc; centre trace) for 10 min. All traces in (e) represent the mean normalised fluorescence intensity (F/F_0) of 100 cells from four separate experiments. Error bars represent S.D. For measurements of basal Mn^{2+} quench (top trace in e) no drugs were added to cultures. (f) Estimated PM potential (E_m) of up to 15 of the closest glial cells to the mechanically stressed target cell which demonstrated an increase in intracellular $DiBAC_4(3)$ fluorescence was averaged for individual experiments of (b), with displayed traces representing the mean of these averaged responses from four separate experiments for untreated control and drug treated cultures (error bars represent S.D.).
←

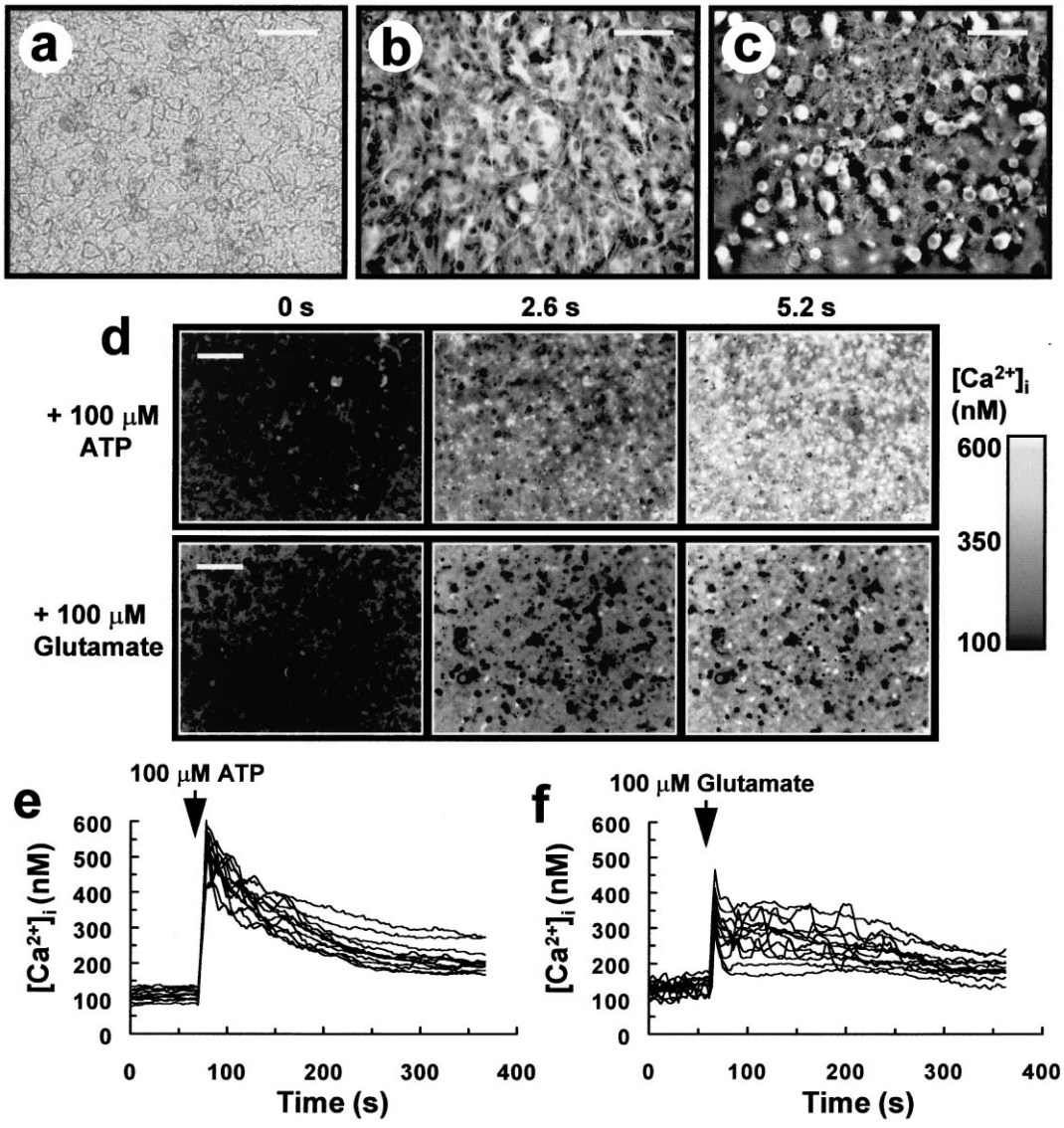

Fig. 4. ATP and glutamate induced elevations in $[Ca^{2+}]_i$ of cells in the PNL of hippocampal organotypic slices. (a) A typical region of the PNL imaged in experiments (microscope illumination). (b,c) Epifluorescence images of glial cells stained with anti-GFAP-oregon green (b) and of neuronal cells stained with anti-NFP-oregon green (c) in similar regions as (a). Scale bars in (a), (b) and (c) are 60 μm. (d) Sequences of fluorescence ratio images of the PNL of hippocampal slices loaded with fura-2, showing elevations in $[Ca^{2+}]_i$ induced by bolus applications of 100 μM ATP or glutamate at $t = 0$ s to the bathing medium. Scale bars in (d) are 120 μm. (e,f) Traces derived from (d) showing typical elevations in $[Ca^{2+}]_i$ of individual cells in the PNL induced by ATP (e) and glutamate (f).

This level of depolarisation should therefore be sufficient to activate high voltage L-type Ca^{2+} channels which open at membrane potentials greater than approximately −35 mV [15]. Several studies have also demonstrated the ability of NO to depolarise mitochondria [16–19], and deplete cellular ATP due to the inhibition of mitochondrial metabolism and glycolysis [19]. In hippocampal neurons these effects were reported to be profound and irreversible at NO concentrations of 2 μM or more [19]. Considering these findings it is possible that NO-induced energy depletion in cells may result in the complete or partial breakdown of transmembrane ion gradient regulation, resulting in PM depolarisation. A complete breakdown of ion gradient regulation by NO may seem unlikely in our study however, as NO-induced elevations in glial $[Ca^{2+}]_i$ were transient (Fig. 1c) and could be regenerated in the same cells by repeated puffs of aqueous NO. These observations indicate that Ca^{2+}-ATPase pumps were still active within the membranes of our cells following multiple NO applications.

As NO synthesis by cNOS is stimulated by treatments that induce an increase in $[Ca^{2+}]_i$ independently of cell surface receptor activation in glia [6], a NO-induced rise in $[Ca^{2+}]_i$ is likely to result in an amplification of NO production. Furthermore, if NO diffusion is unrestricted, subsequent cross-talk between NO and Ca^{2+} could give rise to Ca^{2+} waves, as seen in many single cells and tissues [1]. Our previous observations [6] and data from this study are consistent with such a mechanism operating in glia with NO-induced Ca^{2+} mobilisation [6] and Ca^{2+} influx coupled to PM depolarisation (Fig. 2) seemingly facilitating the propagation of both NO and stress-induced intercellular Ca^{2+} waves. In this study we have also demonstrated that as well as for dissociated glial–neuron cultures, NO can induce slowly propagating intercellular Ca^{2+} waves in hippocampal organotypic slices (Fig. 4).

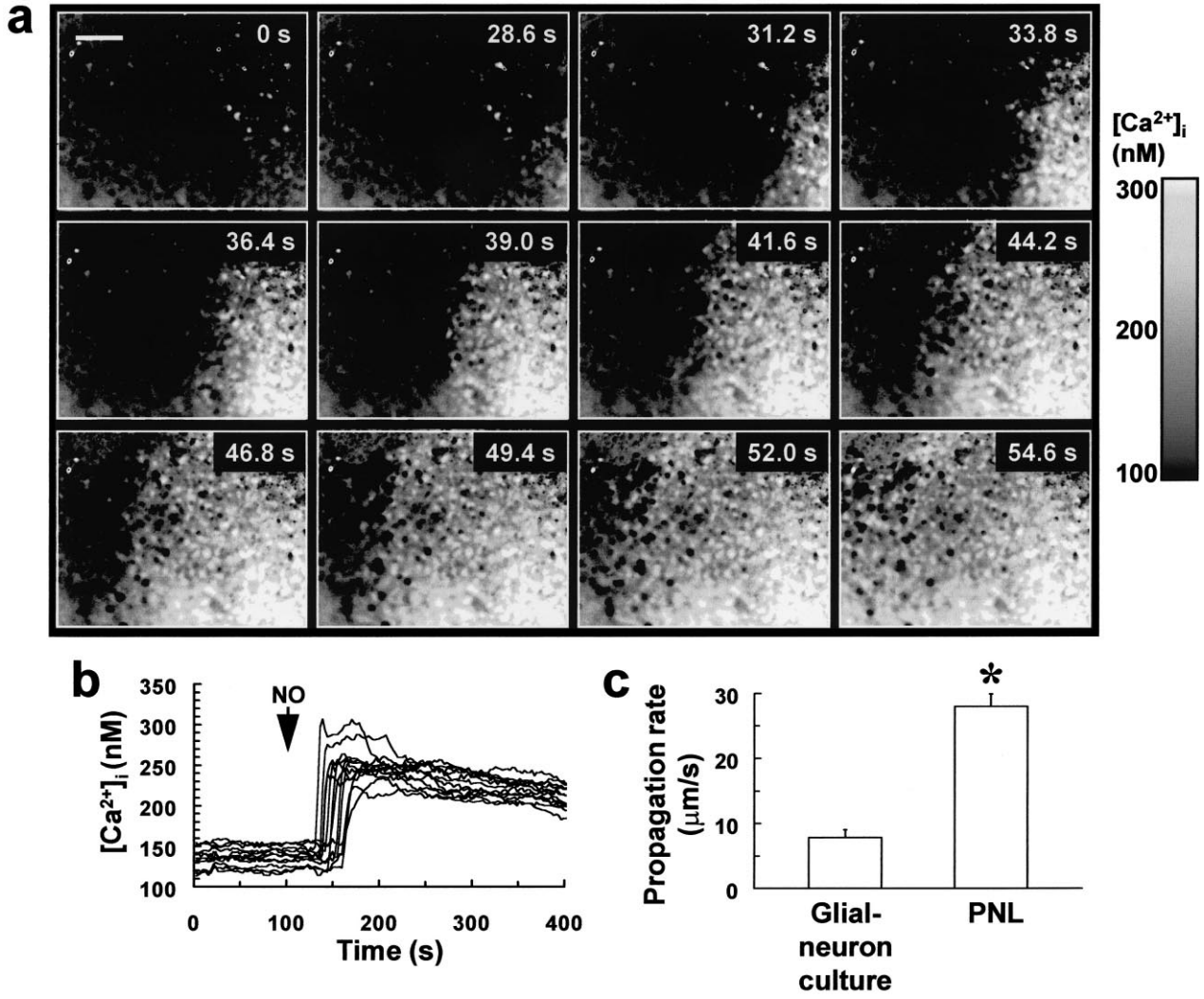

Fig. 5. NO evoked intercellular Ca^{2+} wave in the PNL of a hippocampal organotypic slice. (a) Sequence of fluorescence ratio images of the PNL of a hippocampal slice loaded with fura-2, showing a slowly propagating (from right to left) intercellular Ca^{2+} wave evoked by applying a 5 μl bolus of 350 μM aqueous NO at $t = 0$ s to the bathing medium. The NO bolus was applied at a distance of 1.0 cm from the right hand edge of the slice to a 1 ml volume of bathing medium. Scale bar in (a) is 120 μm. (b) Traces derived from (a) showing typical transient elevations in $[Ca^{2+}]_i$ of individual cells in the PNL which participated in the NO-mediated intercellular Ca^{2+} wave. (c) NO-induced Ca^{2+} waves in the PNL propagate at a faster rate compared to those in dissociated glial–neuron cultures. Bars of (c) are the means of at least three separate estimations, and error bars represent S.D. (*$P < 0.05$ versus glial–neuron culture value; Student's t-test for unpaired observations).

It is therefore tantalising to speculate that NO-mediated intercellular Ca^{2+} waves might play some role in cell–cell communication in the normal functioning brain, or might be implicated in the characteristic spreading neuropathology associated with peri-infarct depolarisations in cerebral ischaemia, where an increased production of NO by cells in the ischaemic core is an important facet [20].

Acknowledgements: We thank HeadFirst, the Golden Charitable Trust, the National Lottery Charities Board, King's Medical Research Trust, and the Royal Society for supporting this work.

References

[1] Berridge, M.J. and Dupont, G. (1994) Curr. Opin. Cell Biol. 6, 267–274.
[2] Nedergaard, M. (1994) Science 263, 1768–1771.
[3] Charles, A.C., Dirksen, E.R., Merill, J.E. and Sanderson, M.J. (1993) Glia 7, 134–145.
[4] Cotrina, M.L., Lin, J.H.C. and Nedergaard, M. (1998) J. Neurosci. 18, 8794–8804.
[5] Guthrie, P.B., Knappenberger, J., Segal, M., Bennett, M.V.L., Charles, A.C. and Kater, S.B. (1999) J. Neurosci. 19, 520–528.
[6] Willmott, N.J., Wong, K. and Strong, A.J. (2000) J. Neurosci. 20, 1767–1779.
[7] Poenie, M. (1990) Cell Calcium 11, 85–91.
[8] Maric, D., Maric, I., Smith, S.V., Serafini, R., Hu, Q. and Barker, J.L. (1998) Eur. J. Neurosci. 10, 2532–2546.
[9] Willmott, N., Sethi, J.K., Walseth, T.F., Lee, H.C., White, A.M. and Galione, A. (1996) J. Biol. Chem. 271, 3699–3705.
[10] Feinstein, D.L., Galea, E., Cermak, J., Chugh, P., Lyandvert, L. and Reis, D.J. (1994) J. Neurochem. 62, 811–814.
[11] Ohta, K., Araki, N., Shibata, M., Hamada, J. and Komatsumoto, S. (1994) Neurosci. Lett. 176, 165–168.
[12] Shaw, P.J., Charles, S.L. and Salt, T.E. (1999) Brain Res. 833, 272–277.
[13] Bains, J.S. and Ferguson, A.V. (1997) Neuroscience 79, 149–159.
[14] Ohkuma, S., Katsura, M., Hibino, Y., Xu, J., Shirotani, K. and Kuriyama, K. (1998) Mol. Brain Res. 54, 133–140.
[15] Janssen, L.J. (1997) Am. J. Physiol. 41, C1757–C1765.
[16] Keelan, J., Vergun, O. and Duchen, M.R. (1999) J. Physiol. 520, 797–813.
[17] Packer, M.A., Miesel, R. and Murphy, M.P. (1996) Biochem. Pharmacol. 51, 267–273.
[18] Almeida, A., Bolanos, J.P. and Medina, J.M. (1999) Brain Res. 816, 580–586.
[19] Brorson, J.R., Schumacker, P.T. and Zhang, H. (1999) J. Neurosci. 19, 147–158.
[20] Iadecola, C. (1997) Trends Neurosci. 20, 132–139.